Electronic Supplementary Material (ESI) for Journal of Materials Chemistry A.

Supporting information

Methylamine driven, non-toxic solvent perovskite growth: moisture assisted fabrication from a novel precursor.

Carlo Andrea Riccardo Perini*[a,b], Anil Reddy Pininti*[a,b], Samuele Martani[a,b], Andrea Perego[c], Daniele Cortecchia[a], Annamaria Petrozza [a] and Mario Caironi [a]

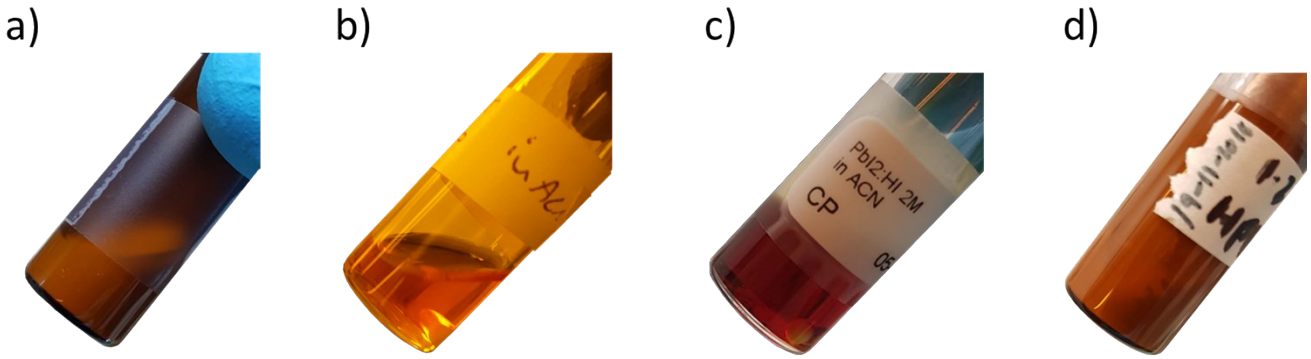

Fig. S 1. From left to right, top to bottom: (a) PbI_2 1M in ACN (it precipitates), (b) PbI_2:HI 1M in ACN (fully solvated), (c) PbI_2:HI 2M in ACN, (d) $HPbI_3$, synthesized as reported in Ref. 1 (not solubilized in ACN).

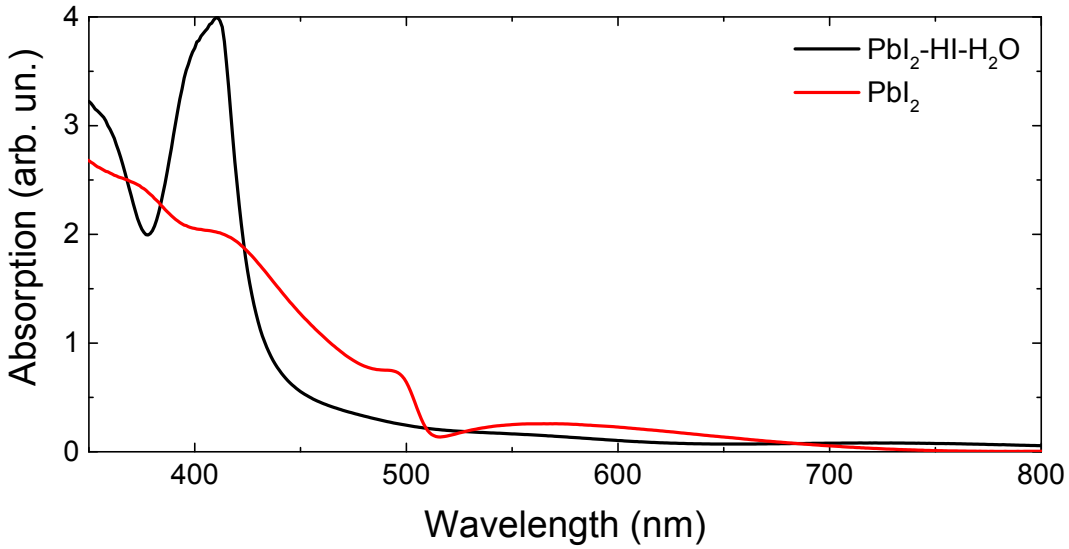

Fig. S 2. absorption profile of PbI_2 and PbI_2-HI-H_2O.

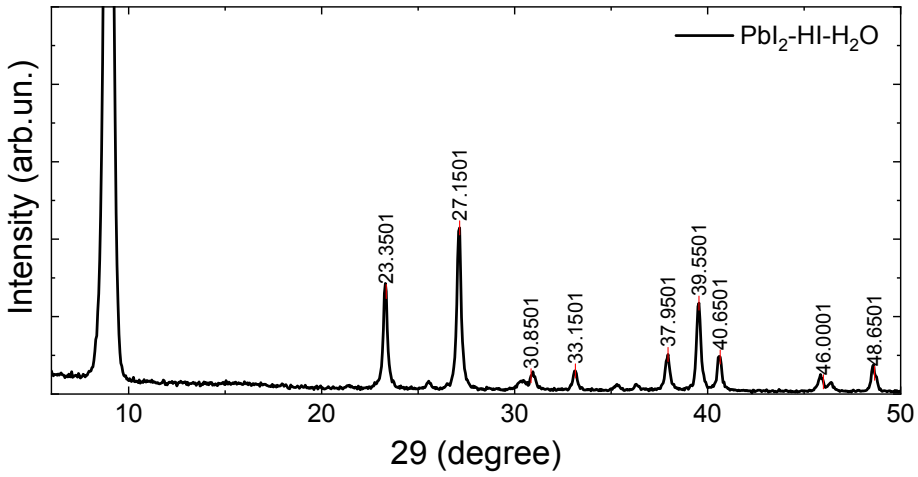

Fig. S 3. Zoom in of the XRD pattern of the PbI_2-HI-H_2O precursor. Main peak positions are highlighted.

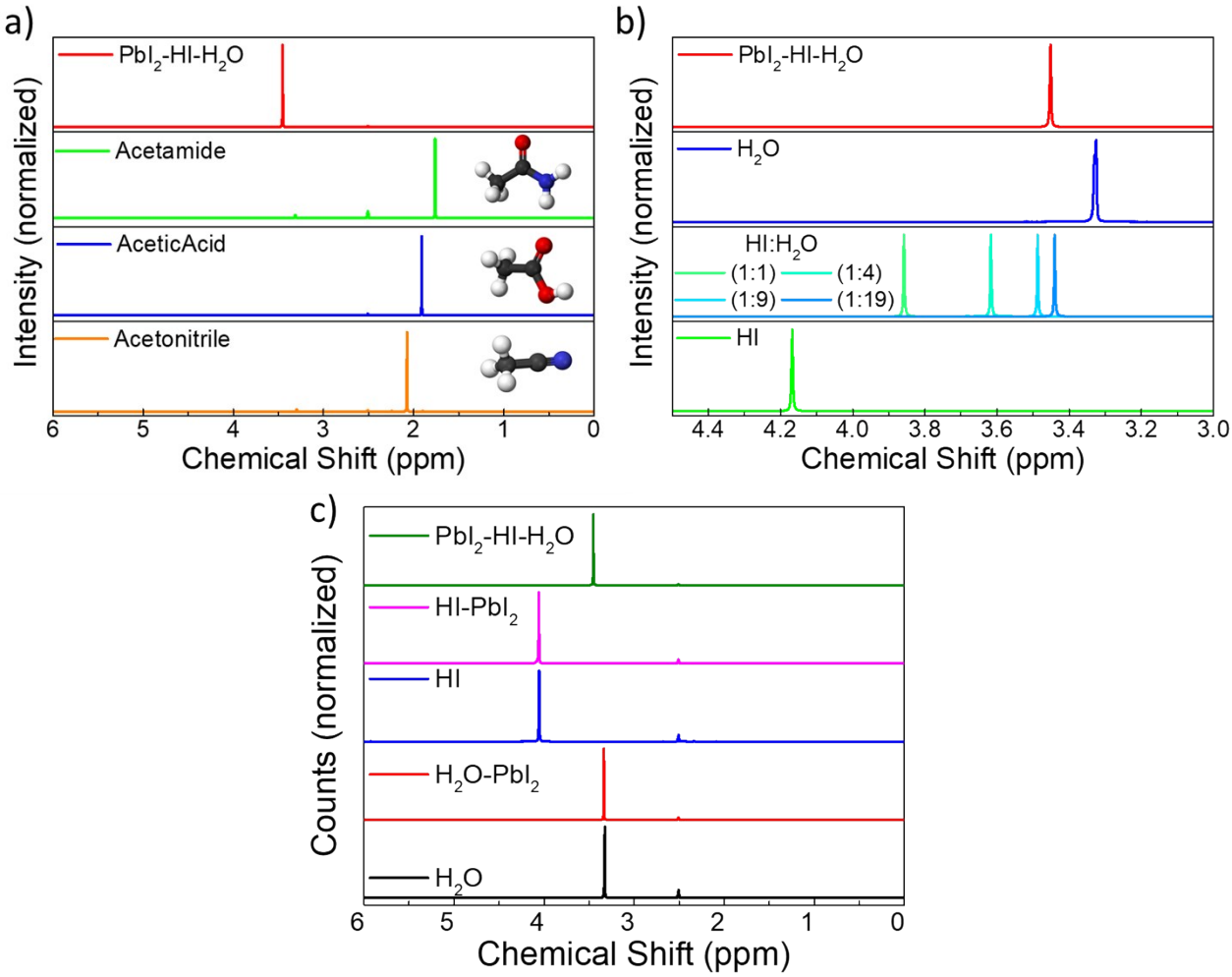

Fig. S 4: (a) ^{1}H NMR spectra of the as spun PbI_2-HI-H_2O precursor dissolved in deuterated-DMSO, compared with ^{1}H NMR of Acetonitrile, Acetamide and Acetic Acid. The chemical structures of the solvents are presented in the inset (H-white, O-red, N-blue, C-black). (b) Chemical shift of PbI_2-HI-H_2O compared with water at different pH conditions. The presented ratios refer to the volume of HI-solution to

volume of H_2O used. (c) ^1H NMR spectra of PbI_2:HI (1:1 M), H_2O:PbI_2 (1:1 M), HI and H_2O compared with the spectra of the PbI_2-HI-H_2O precursor film.

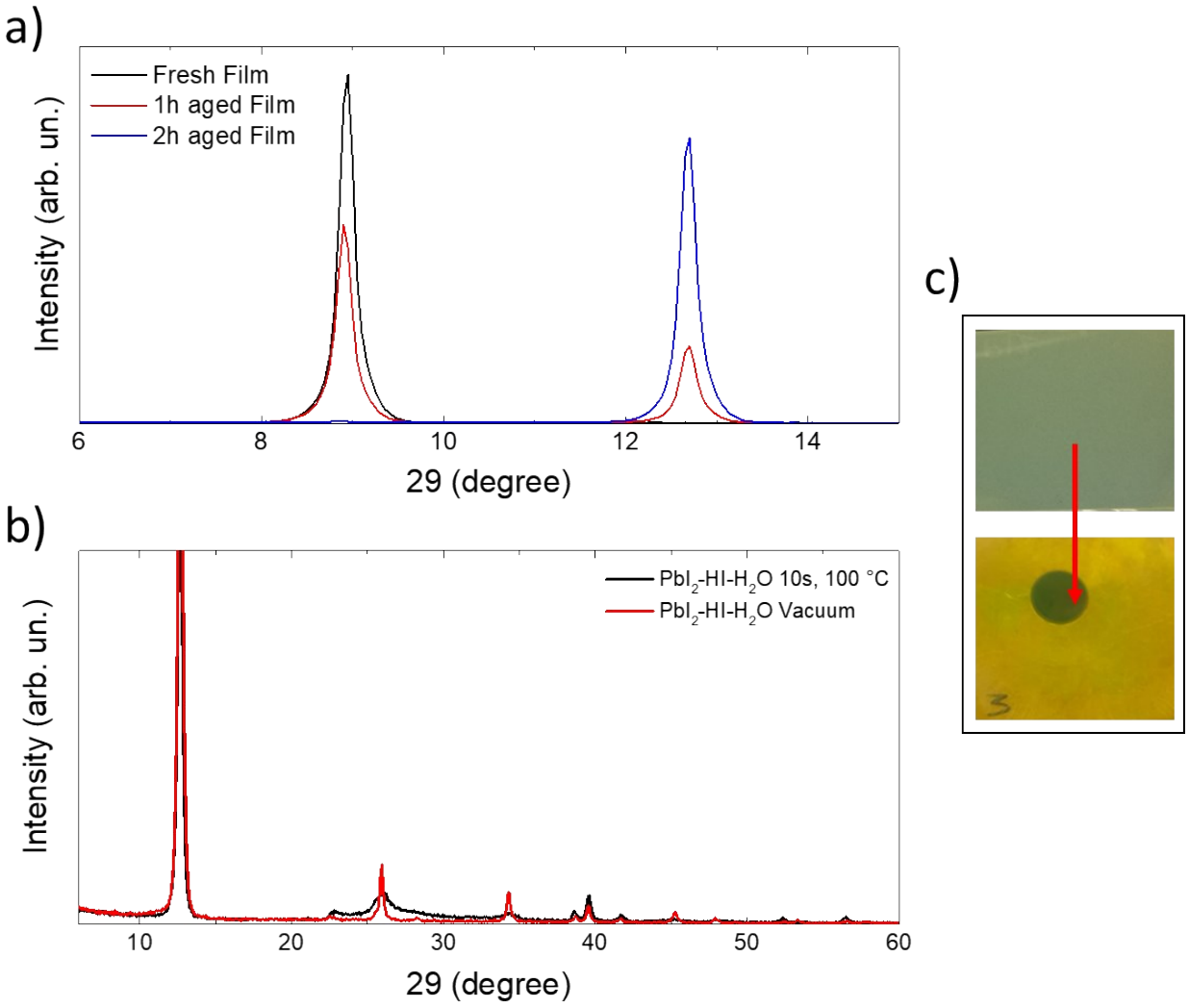

Fig. S 5. (a) Evolution of the as prepared PbI_2-HI-H_2O precursor at low moisture levels (<50 % RH) and 23 °C. The material reverts to PbI_2 within 2 hours of time. (b) Precursor degradation upon exposure to heat (10s, 100°C) or low vacuum (1 cycle, Glove-box antechamber). (c) An image of the deposited film, before and after degradation via heat treatment.

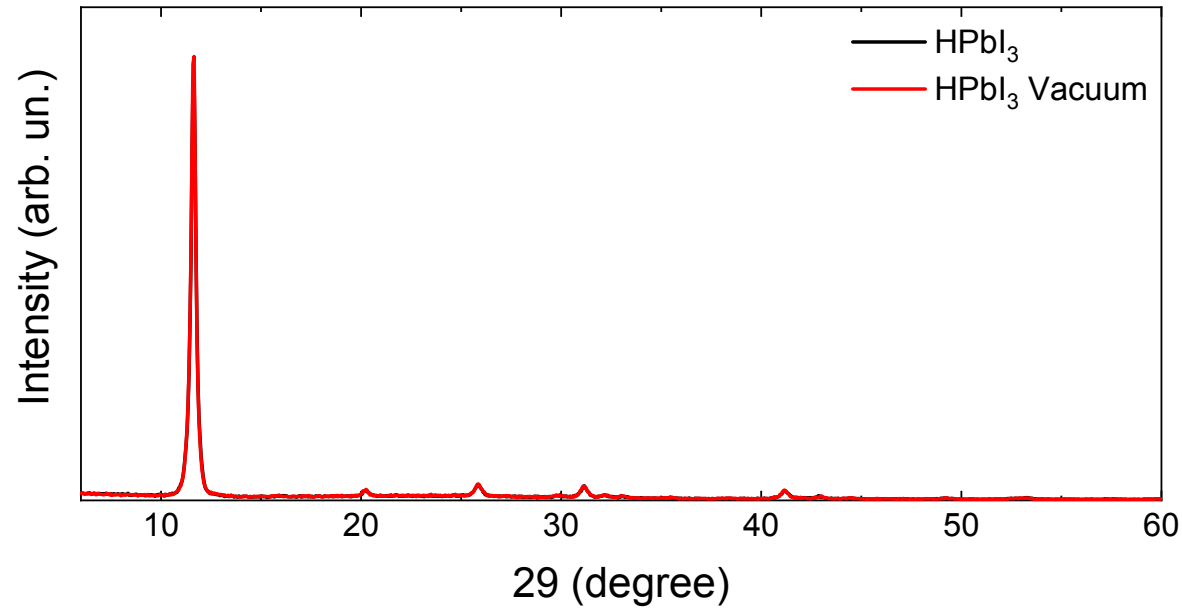

Fig. S 6. $HPbI_3$ film deposited from DMF, no variations in the crystalline structure are observed after placing the samples in low vacuum (Glove-box antechamber – 5 min).

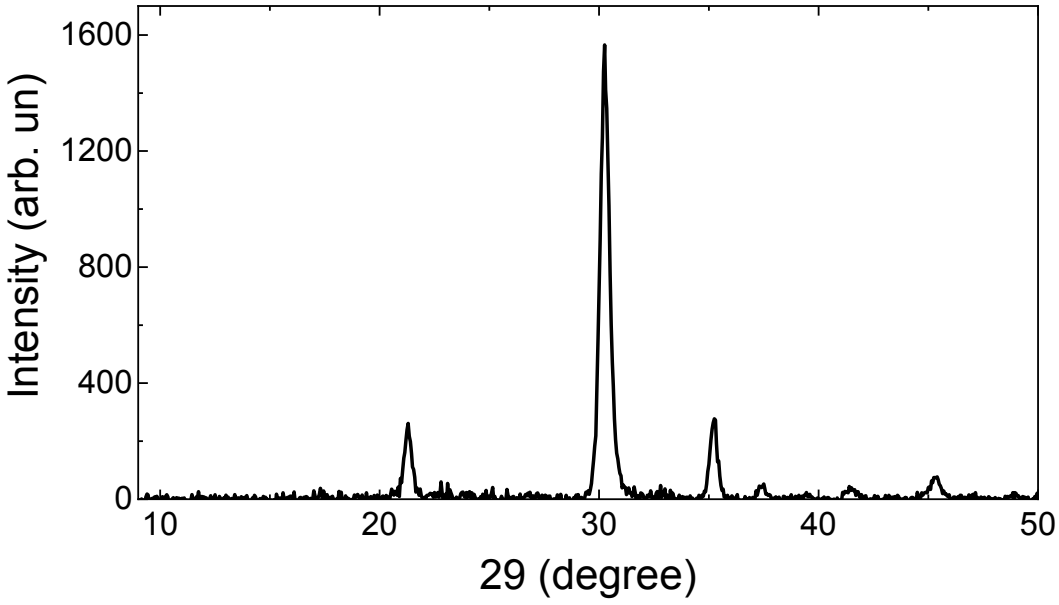

Fig. S 7. XRD of the ITO/PEDOT:PSS substrate.

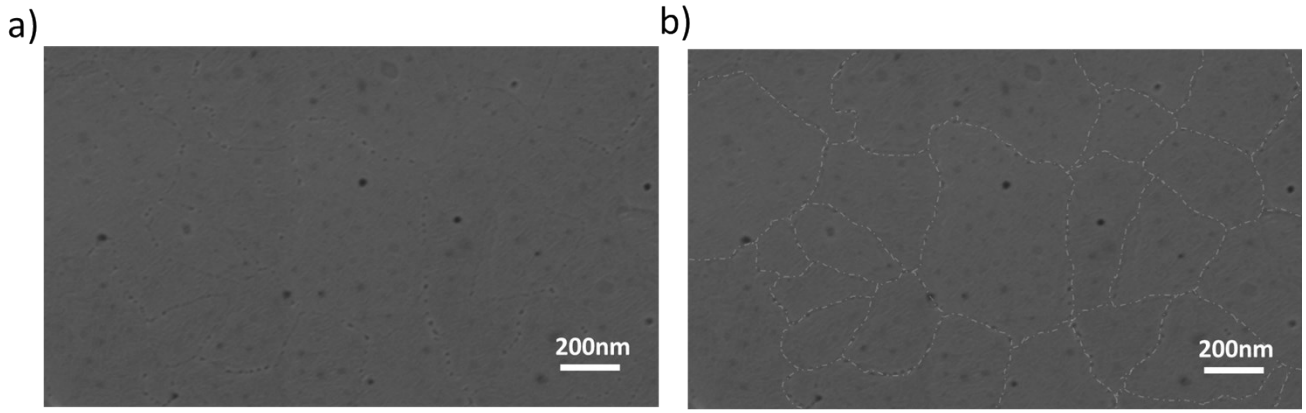

Fig. S 8. a) High resolution top-view SEM image of a perovskite film processed at 65 % RH. Low contrast grain boundaries are visible and are highlighted in (b).

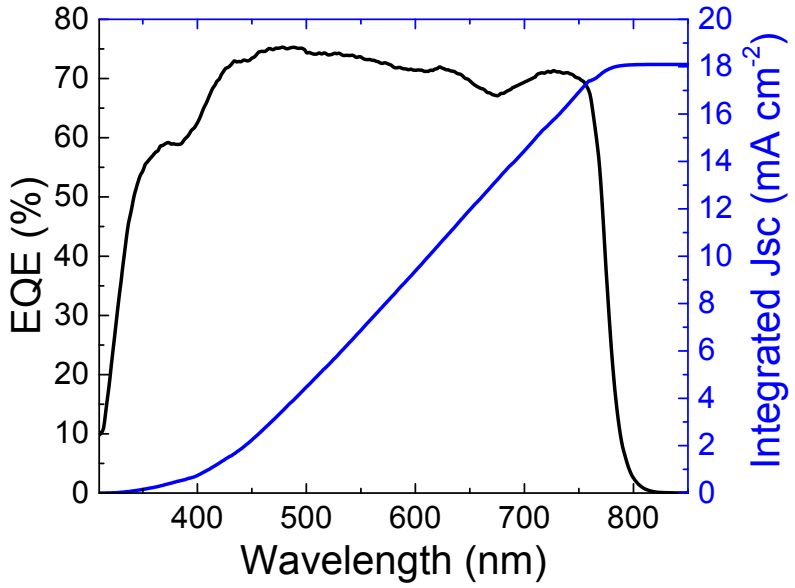

Fig. S 9. EQE spectra and integrated Jsc of the device presented in Fig. 4e. Good Match is observed between the measured and the integrated current.

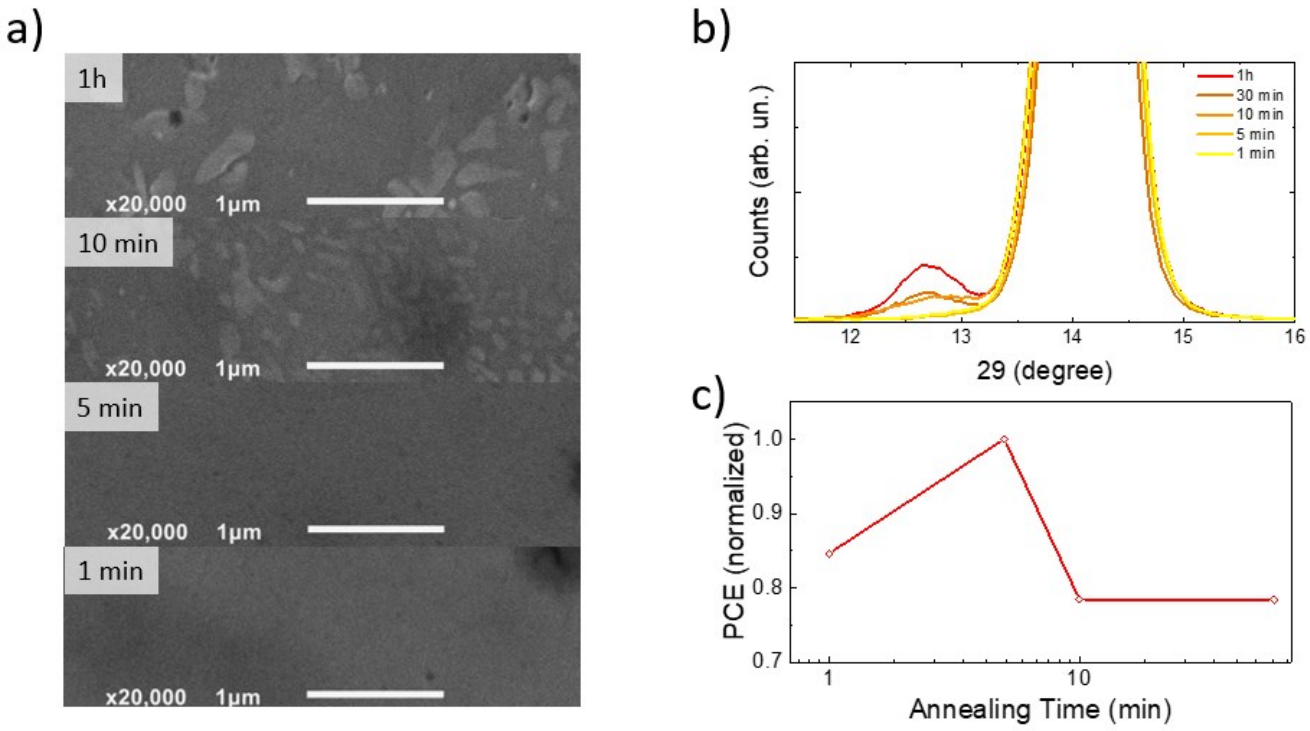

Fig. S 10: $MAPbI_3$ SEM top view (a), XRD (b) and PCE (c) evolution upon exposure to increasing annealing time. Best performances are obtained with a 5 min annealing time.

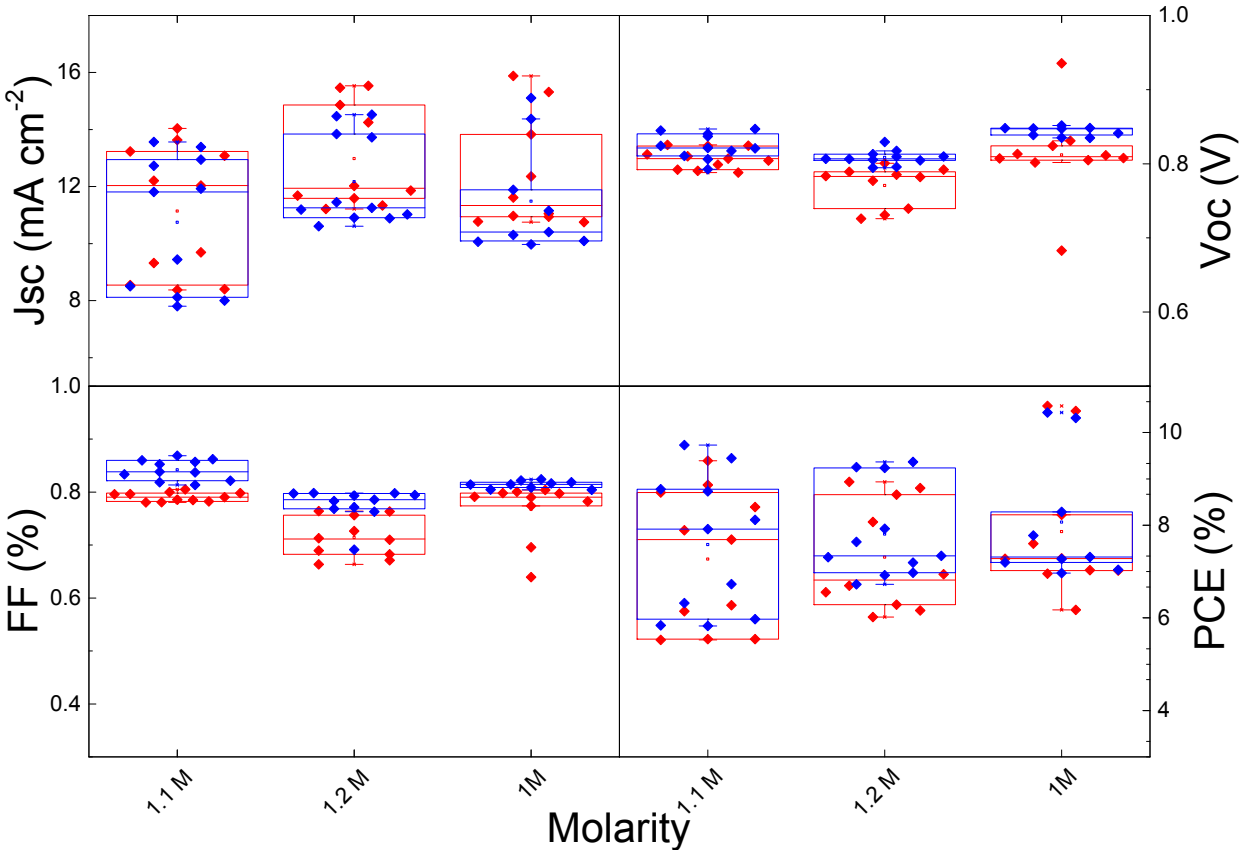

Fig. S 11. Device performance distribution of devices fabricated at 75 % RH from PbI_2-HI-H_2O solutions with different molarity. Notably, the current densities and the fill factors of the devices are not impacted by an increase in the concentration of the precursor solution (which corresponds to thicker films).

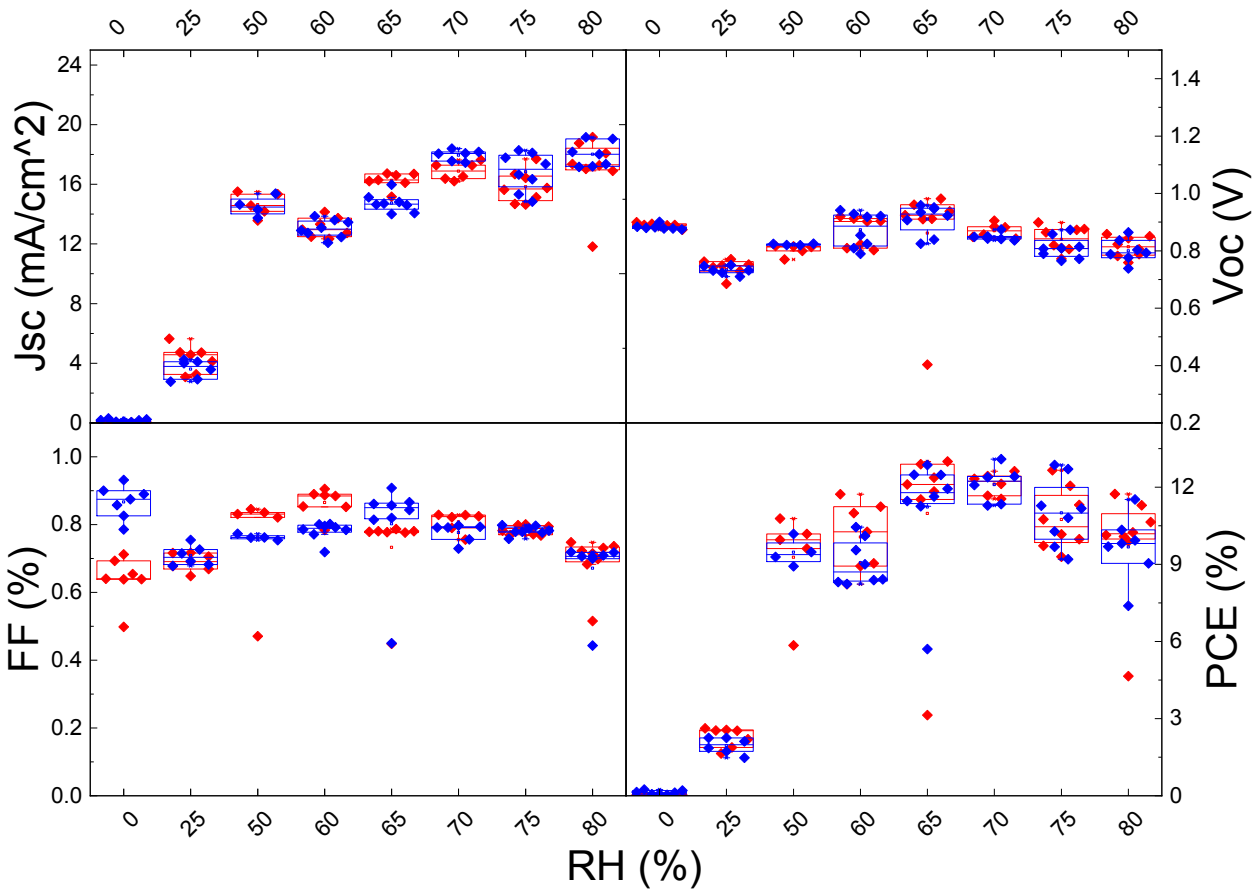

Fig. S 12. Figures of merit distribution for devices fabricated at different moisture levels. 0 RH % corresponds to samples processed in glovebox.

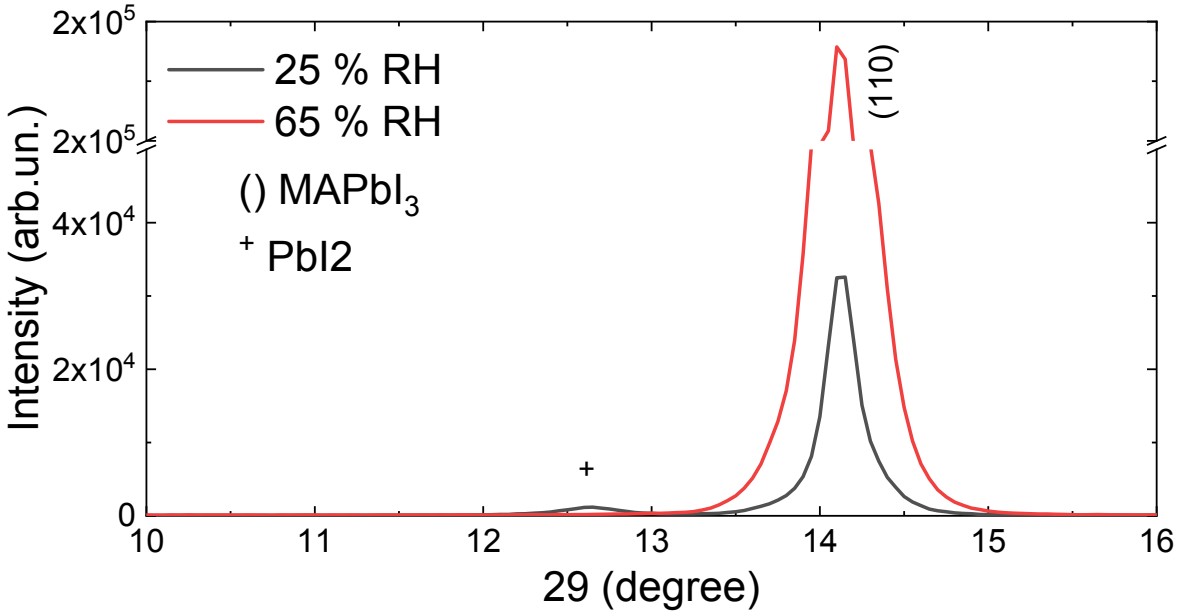

Fig. S 13. XRD of MA-PVK films processed at 25 % RH and 65 % RH.

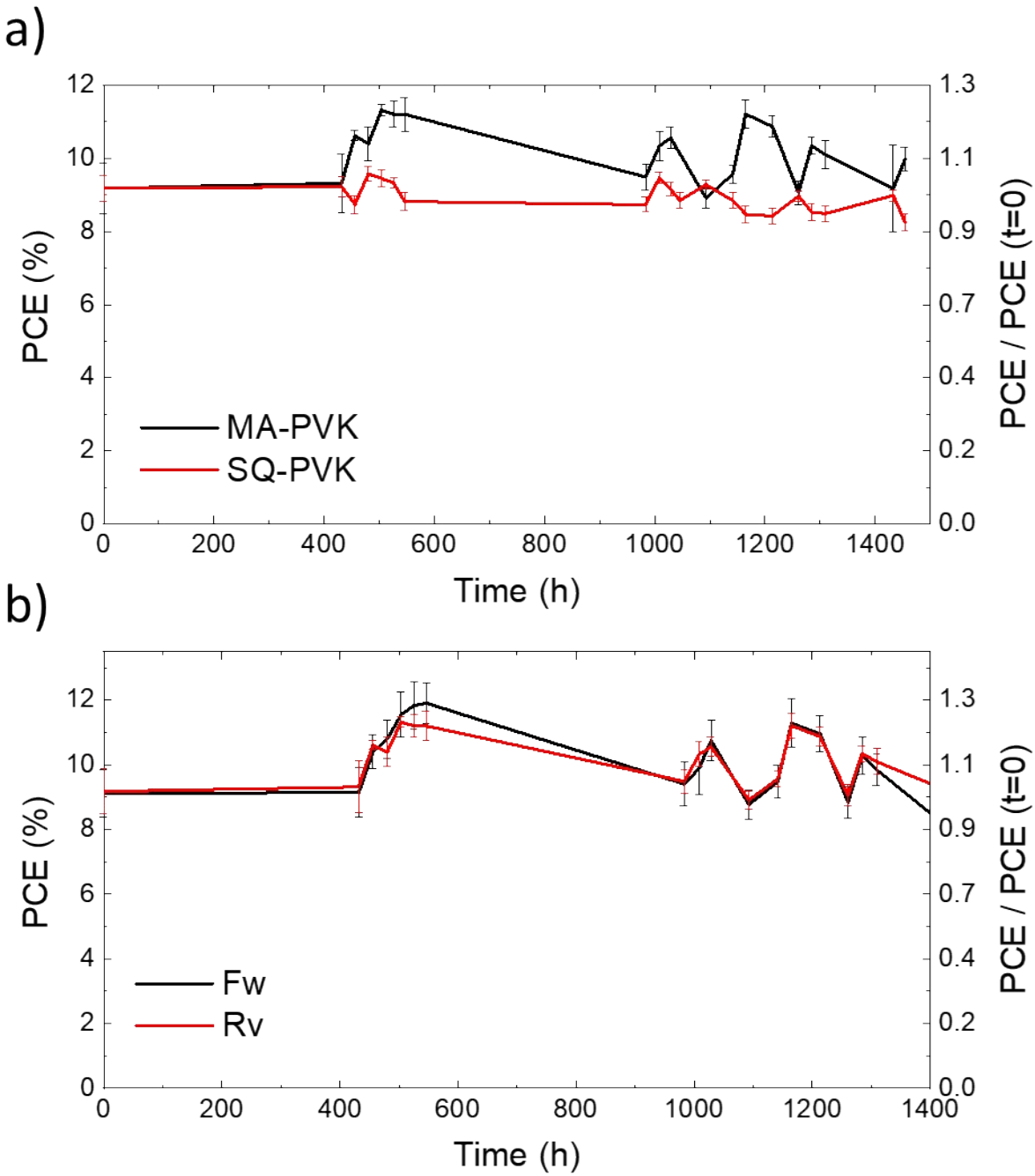

Fig. S 14. a) Shelf Life stability of a MA-PVK solar cells processed at 76 % RH compared with cells based on SQ-PVK. Results are averaged over 4 devices each. b) Forward and reverse scan performance evolution of the MA-PVK based solar cell. Devices are stored in nitrogen environment and exposed to AM1.5 illumination in air during the measurement.

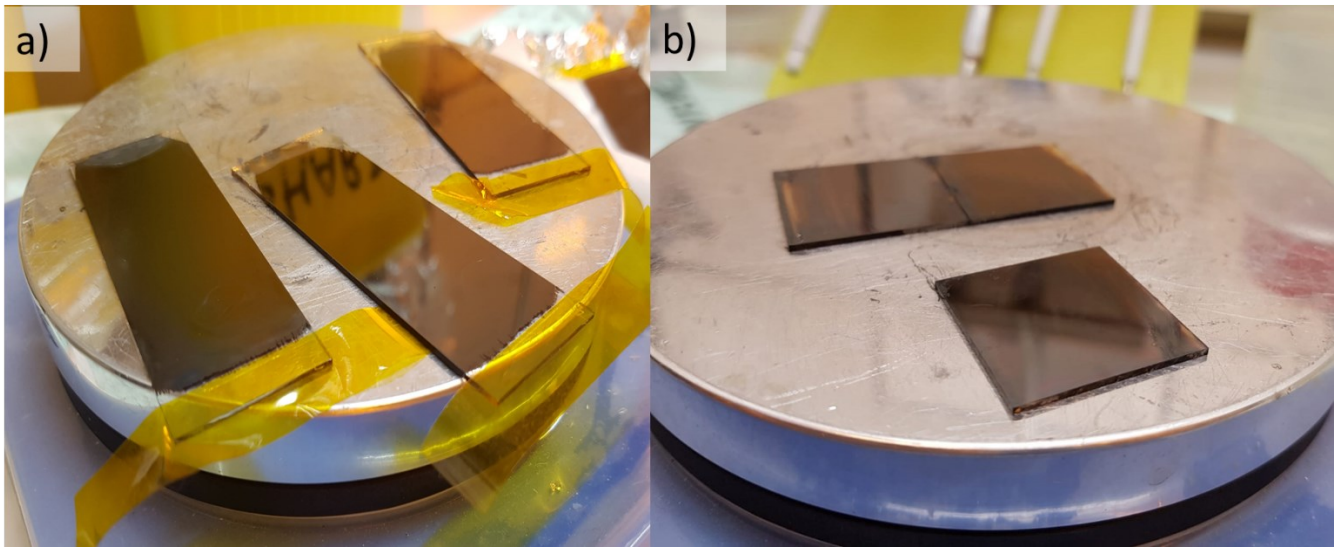

Fig. S 15. a) MA-PVK deposited via blade coating on 7.5 cm x 2.5 cm glass slides. b) MA-PVK deposited by blade coating on 2.54 cm x 2.54 cm Glass/ITO substrates.

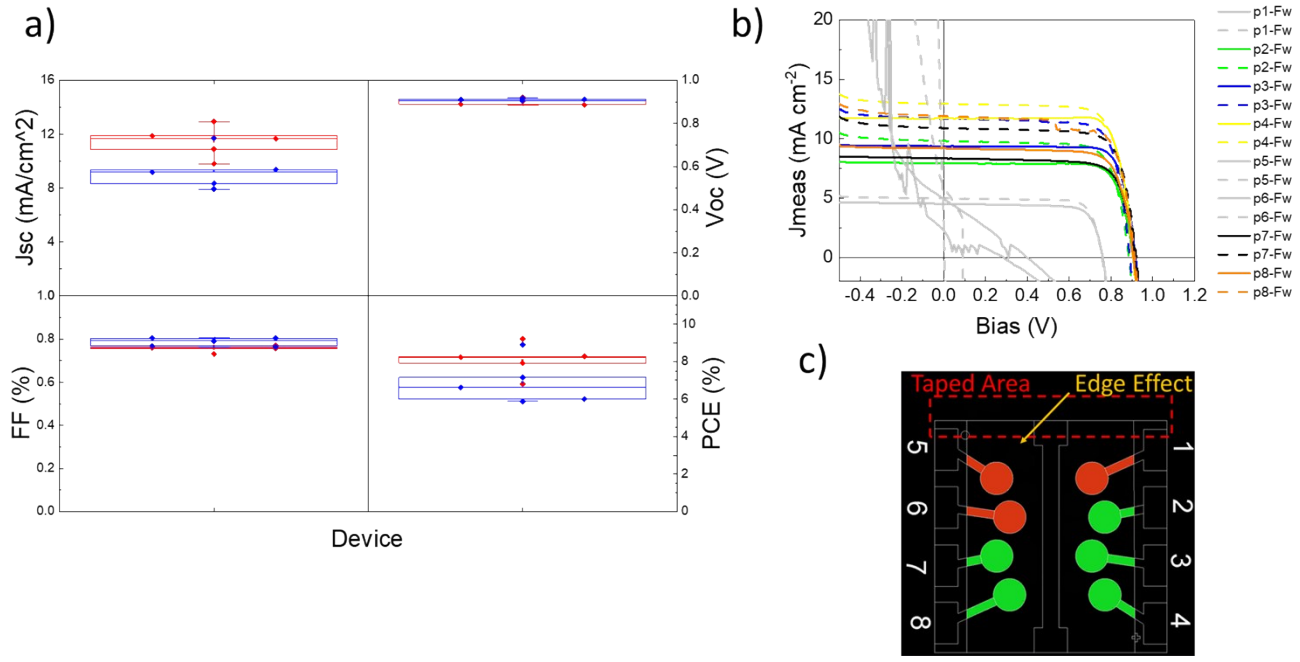

Fig. S 16. a) Performance distribution for selected pixels (green in figure c) processed on the same substrate. b) J-V scans of solar cells processed on the same 2.54 cm x 2.54 cm substrate. c) Pixel position with respect to the blade coating process. Some pixels are lost due to the use of tape to hold the substrate during the coating process and to non-uniform coverage at the tape edge where the scan starts. After this initial threshold, all remaining pixels over a >3 cm^2, are proved to work.

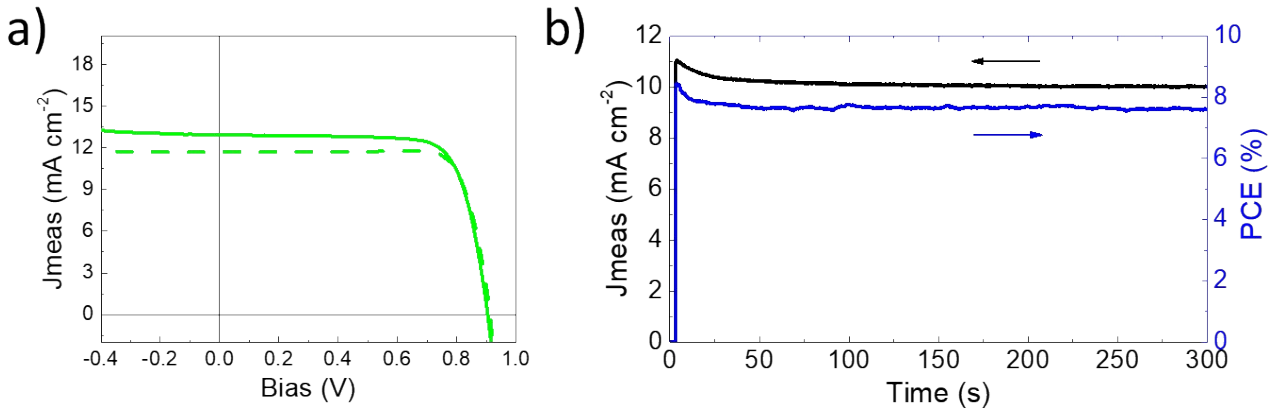

Fig. S 17. a) Forward (solid) and reverse (dashed) J/V scans of a solar cell device with blade coated $MAPbI_3$. b) Maximum Power Point Tracking stabilization of the device under 1 Sun illumination.

Year	HTL	ETL	Perovskite	PCE [%]	T [°C]	Atm.	RH [%]	Mode	Store	Meas. Delay [h]	T80 [h]	Encapsulated	Ref.
2019	ITO/PEDOT:PSS	PCBM/Ag	$MAPbI_3$	10.3	10-20	Air	20-40	jV	Dark	120	216	No?	[2]
2019	ITO/PEDOT:PSS	PCBM/BCP/Ag	$MAPbI_3$	15.05	RT	DryBox	0	JV	Dark	24	408	No?	[3]
2019	ITO/PEDOT:PSS	PCBM/Ag	$MAPbI_3$	16.5	?	?	?	?	?	?	?	?	[4]
2019	ITO/PEDOT:PSS	PCBM/Ag	$MAPbI_3$	17.2	RT	?	?	JV	Dark	50-192	432	no	[5]
****	\\	\\	\\	\\	\\	\\	\\	MPPT?	Light	?	20	no	[5]
2018	ITO/PEDOT:PSS	PCBM/ZnO-nps/Ag	$MAPbI_{3-x}Br_x$	15	RT	Air	?	JV	?	12	90	yes	[6]
2018	ITO/PEDOT:PSS	PCBM/Bphen/Ag	$MAPbI_3$	12	20	Air	45	JV	Dark	50	100	No	[7]
2018	ITO/PEDOT:PSS	PCBM/bis-C60/Ag	$MAPbI_3$	13	RT	DryBox	20	JV	Dark	24	312	No	[8]
2018	ITO/PEDOT:PSS	PCBM/RhB101/LiF/Ag	$MAPbI_{3-x}Cl_x$	13	RT	Air	55	JV	Dark	50	15	no	[9]
2018	FTO/PEDOT:PSS	PCBM/Ag	$MAPbI_3$	13	25	Air	30-50	JV	Dark	24	200	yes	[10]
2018	ITO/PEDOT:PSS	PCBM/BCP/Ag	$MAPbI_3$	12	RT	Air	30-60	JV	Dark	200-1000	600	no	[11]
2017	ITO/PEDOT:PSS	PCBM/Ag	$MAPbI_3$	11.9	RT	Air	15	JV	Dark	24-192	100	no	[12]
2017	ITO/PEDOT:PSS	$PC_{71}BM$/Ca/Al	$MAPbI_3$	20	85	Air	85	JV	Light	120	24	yes	[13]
****	\\	\\	\\	\\	RT	GBox	0	JV	Dark	?	>720	yes	[13]
2017	ITO/PEDOT:PSS	PCBM/LiF/Al	$MAPbI_{3-x}Cl_x$	10.5	?	Air	?	JV-held@Jsc	Light	Cont.	25	yes	[14]
****	\\	\\	\\	\\	18	Air	32	JV	Dark	180-300	400	yes	[14]
2015	ITO/PEDOT:PSS	PCBM/C60/Ag	$MAPbI_3$	11	RT	Air	?	JV	Dark	12-50	90	np	[15]
2015	PEDOT:PSS	PCBM/PTCDI/Cr_2O_3/Cr/Au	$MAPbI_3$	12	RT	Air	?	MPPT	Light		56	no	[16]
2015	ITO/PEDOT:PSS	PCBM/Al	$MAPbI_3$	12.8	25	Air	30-50	JV	Dark?	12-288	1	no	[17]
2015	ITO/PEDOT:PSS	PCBM/Ca/Al	$MAPbI_3$	18	RT	Gbox	0	JV	Dark	120	1080	No	[18]
****	\\	\\	\\	\\	\\	\\	0	JV	Light	50	>144	no	[18]
2015	ITO/PEDOT:PSS	PCBM/Au	$MAPbI_3$	18.1	?	?	40-70	JV	Dark	50	336	no	[19]
2015	ITO/PEDOT:PSS	C60/B-phen/Ag	$MAPbI_3$	12	25	Air	30	JV	Dark	24	180	No	[20]

Table S 1. Overview of reported stability characterization protocols for MAPbX3 -based inverted solar cells including a PEDOT:PSS hole transporting layer.

References

1 M. Long, T. Zhang, Y. Chai, C. F. Ng, T. C. W. Mak, J. Xu and K. Yan, *Nat. Commun.*, 2016, **7**, 1–11.

2 Y. Zhu, S. Wang, R. Ma and C. Wang, *Sol. Energy*, 2019, **188**, 28–34.

3 W. Hu, C. Y. Xu, L. Bin Niu, A. M. Elseman, G. Wang, D. B. Liu, Y. Q. Yao, L. P. Liao, G. D. Zhou and Q. L. Song, *ACS Appl. Mater. Interfaces*, 2019, **11**, 22021–22027.

4 K. Jiang, F. Wu, G. Zhang, P. C. Y. Chow, C. Ma, S. Li, S. Wong Kam, L. Zhu and H. Yan, *J. Mater. Chem. A*, , DOI:10.1039/c8ta12232f.

5 D. Yang, X. Zhang, K. Wang, C. Wu, R. Yang, Y. Hou, Y. Jiang, S. Liu and S. Priya, *Nano Lett.*, 2019, **19**, 3313–3320.

6 J. C. Yu, J. A. Hong, E. D. Jung, D. Bin Kim, S. Baek, S. Lee, S. S. Park, K. J. Choi and M. H. Song, *Sci. Rep.*, 2018, 3–11.

7 P. Fan, D. Zheng, Y. Zheng and J. Yu, *Electrochim. Acta*, 2018, **283**, 922–930.

8 Q. Wang, C. C. Chueh, M. Eslamian and A. K. Y. Jen, *ACS Appl. Mater. Interfaces*, 2016, **8**, 32068–32076.

9 L. Hu, M. Li, K. Yang, Z. Xiong, B. Yang, M. Wang, X. Tang, Z. Zang, X. Liu, B. Li, Z. Xiao, S. Lu, H. Gong, J. Ouyang and K. Sun, *J. Mater. Chem. A*, 2018, **6**, 16583–16589.

10 S. Ma, W. Qiao, T. Cheng, B. Zhang, J. Yao, A. Alsaedi, T. Hayat, Y. Ding, Z. Tan and S. Dai, *ACS Appl. Mater. Interfaces*, 2018, **10**, 3902–3911.

11 P. Fassl, V. Lami, A. Bausch, Z. Wang, M. T. Klug, H. J. Snaith and Y. Vaynzof, *Energy Environ. Sci.*, 2018, **11**, 3380–3391.

12 H. Luo, X. Lin, X. Hou, L. Pan, S. Huang and X. Chen, *Nano-Micro Lett.*, 2017, **9**, 1–11.

13 C. H. Chiang, M. K. Nazeeruddin, M. Grätzel and C. G. Wu, *Energy Environ. Sci.*, 2017, **10**, 808–817.

14 C. Bracher, B. G. Freestone, D. K. Mohamad, J. A. Smith and D. G. Lidzey, *Energy Sci. Eng.*, 2018, **6**, 35–46.

15 J. H. Kim, P. W. Liang, S. T. Williams, N. Cho, C. C. Chueh, M. S. Glaz, D. S. Ginger and A. K. Y. Jen, *Adv. Mater.*, 2015, **27**, 695–701.

16 M. Kaltenbrunner, G. Adam, E. D. Głowacki, M. Drack, R. Schwödiauer, L. Leonat, D. H. Apaydin, H. Groiss, M. C. Scharber, M. S. White, N. S. Sariciftci and S. Bauer, *Nat. Mater.*, 2015, **14**, 1032–1039.

17 J. You, L. Meng, T.-B. Bin Song, T.-F. F. Guo, W.-H. H. Chang, Z. Hong, H. Chen, H. Zhou, Q. Chen, Y. Liu, N. De Marco, Y. Yang, W.-H. H. Chang, Z. Hong, H. Chen, H. Zhou, Q. Chen, Y. Liu and N. De Marco, *Nat. Nanotechnol.*, 2016, **11**, 75–81.

18 C. G. Wu, C. H. Chiang, Z. L. Tseng, M. K. Nazeeruddin, A. Hagfeldt and M. Grätzel, *Energy Environ. Sci.*, 2015, **8**, 2725–2733.

19 J. H. Heo, H. J. Han, D. Kim, T. K. Ahn and S. H. Im, *Energy Environ. Sci.*, 2015, **8**, 1602–1608.

20 F. Hou, Z. Su, F. Jin, X. Yan, L. Wang, H. Zhao, J. Zhu, B. Chu and W. Li, *Nanoscale*, 2015, **7**, 9427–9432.